

Network reconstruction of platelet metabolism identifies metabolic signature for aspirin resistance

Alex Thomas^{1,4}, Sorena Rahmanian^{2,4}, Aarash Bordbar^{2,4}, Bernhard Ø. Palsson^{2,3,4}, Neema Jamshidi^{3,4,5,6}

1: Department of Bioinformatics

2: Department of Bioengineering

3: Institute of Engineering and Medicine

4: University of California, San Diego

9500 Gilman Drive, Mail Code 0412

La Jolla, CA 92093-0412

5: Department of Radiological Sciences

University of California, Los Angeles, BOX 951721

Los Angeles, CA 90095-1721

6: Corresponding author: neema@ucsd.edu

Supplemental Material

1. Figures (network maps zoomable up to 6400%)
2. Figure Legends
3. Supplemental Data File Legends
4. Methods
5. References

FIGURE LEGENDS

Figure S1. Comparison of the size of the platelet reconstruction, iAT-PLT-636, to other network reconstructions. A. The platelet is the smallest human cell and according to biochemical content its complexity fits between the mature erythrocyte and the macrophage (two other cells of hematopoietic lineage). Other human cell or tissue-specific reconstructions have more content, as expected, but all follow along the same trend. The scope and characterization of these networks biases (and underestimates) the actual size and complexity of human cells, as noted by the comparative sizes *E. coli* and yeast ¹⁻⁵, which are larger than human cells due to the comparative level of detailed knowledge of their underlying biochemical content and capabilities. B. A more detailed comparison between the platelet, red cell, and macrophage highlight some of the differences in content based on canonical metabolic subsystems.

Figure S2. Significant (Wilcoxon signed rank-sum test, $p<0.05$) flux fold differences of reactions between the ASA-r and ASA-s conditions. Blue reactions indicate fluxes that have an average higher flux in the ASA-s phenotype, red reactions indicate fluxes that have higher flux in the ASA-r phenotype. The full reaction map of the platelet is shown. Significant left null space balances are shown to the right of the reaction map.

Figure S3. Significant (Wilcoxon signed rank-sum test, $p<0.05$) flux fold differences of reactions between the ASA-r and ASA-s conditions, with redox load. Blue reactions indicate fluxes that have an average higher flux in the ASA-s phenotype, red reactions indicate fluxes that have higher flux in the ASA-r phenotype. This figure is the full reaction map that is previewed in Figure 3A.

Figure S4. The full platelet reaction map. This is the reaction map that is used in figures 3A, S3, and S4.

Figure S5: Contrasting how to calculate coupling sets to calculating directional coupling as per the definition of ⁶.

DATA FILE LEGENDS

Data File S1. Drug enrichment analysis and annotations.

Data File S2. iAT-PLT-636 references, annotations, and content.

Data File S3. Enumeration of coupled reaction sets and cosets in iAT-PLT-636

Data File S4. ASA-s and ASA-r sampling constraints and comparisons.

platelet.xml: SBML format of iAT-PLT-636

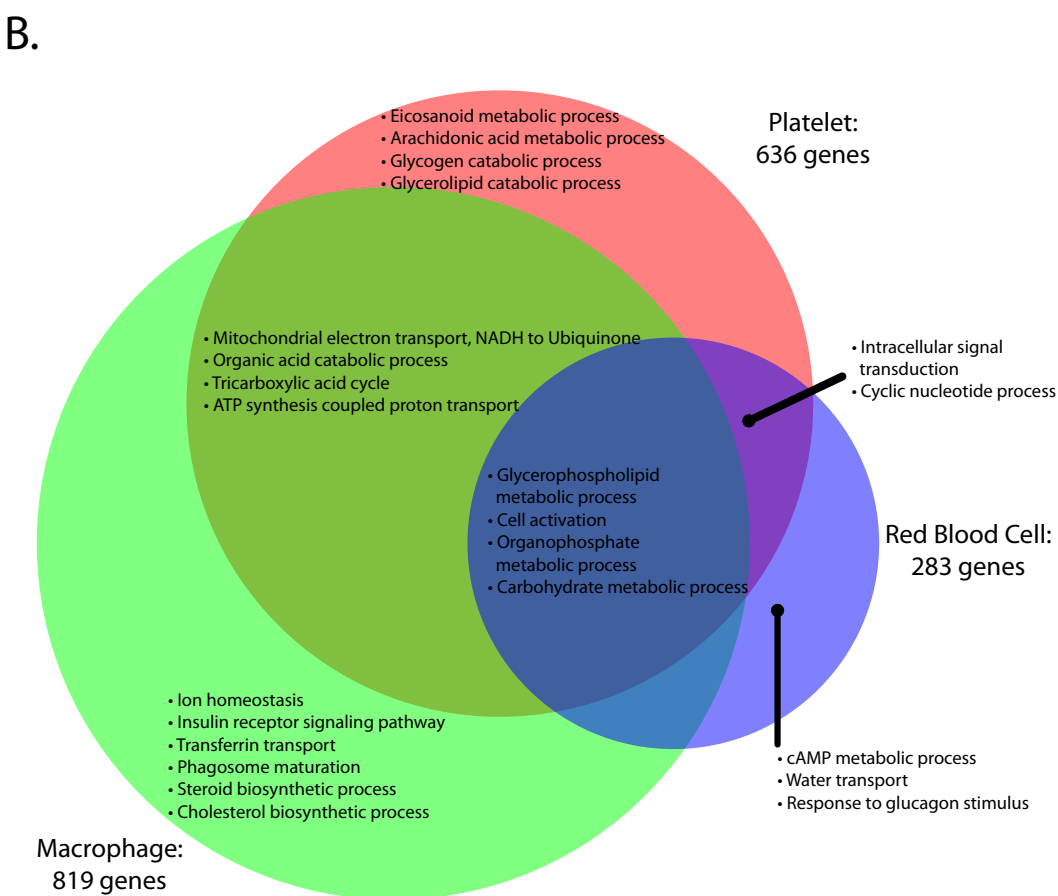
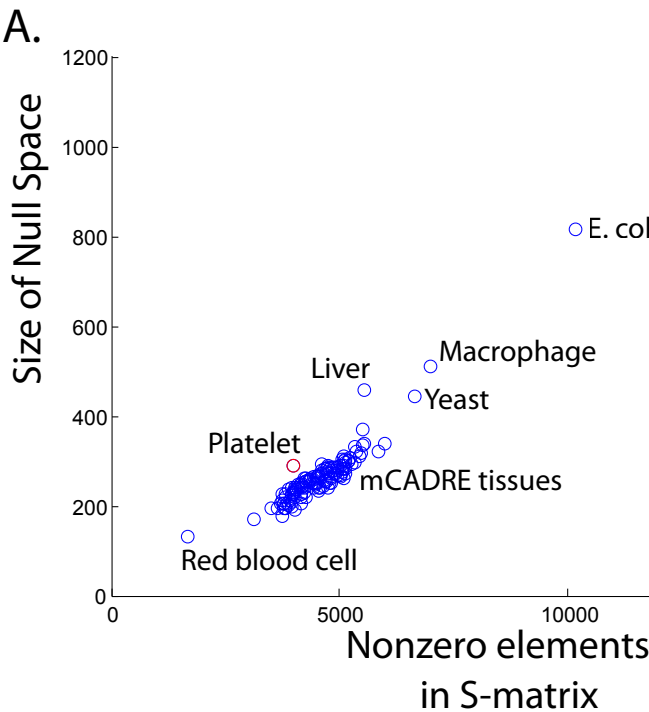
platelet_loopless.xml: SBML format of iAT-PLT-636 (with type III loops removed)

SUPPLEMENTAL METHODS

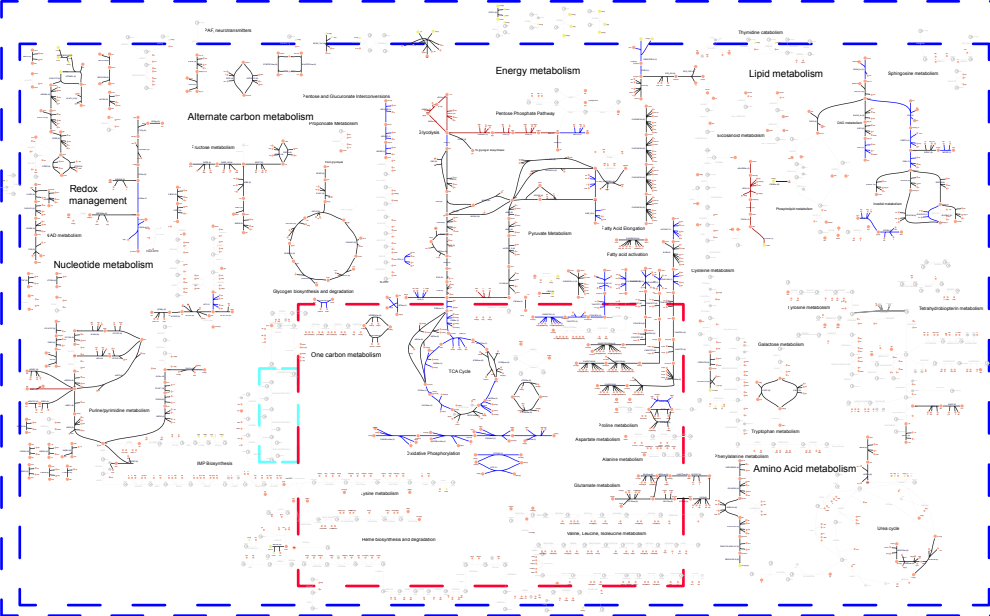
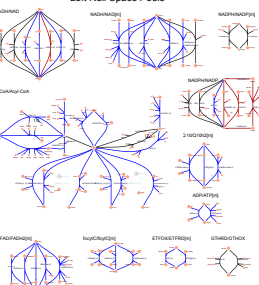
The coupling sets that were calculated for the reaction connectivity in the platelet metabolic model were primarily motivated by flux coupling analysis^{6,7} and master/slave relations⁸. The method for calculating coupled sets was derived from what was used to calculate master/slave relations. Kim & Motter defined the master reaction and slave reactions based on achieving a unique flux for v_j , as in $v_{min,j}$ equals $v_{max,j}$, but our approach allows any constraining of the flux from the minimum and maximum values of v_j to be denoted as “coupling”. Note that this does not imply controllability of reactions and the relationship is bi-directional, two differences from Kim & Motter’s approach⁸. Flux coupling analysis has more stringent rules for determining coupling, although fully coupled reactions are synonymous to hard coupled, correlated reaction sets (Figure S5). Specifically, there are no partial coupling for the platelet model when conducting coupling analysis with open constraints (R_{min} can never be non-zero), and any directional coupling between reactions is counted as “coupling” in our analysis (Figure S5). Due to less stringent criteria for inclusion of a reaction in a coupling set, the resulting analysis is inclusive of the two previous approaches to define reaction connectivity in the platelet model and was able to present the most complete picture for reaction connectivity in the model.

REFERENCES

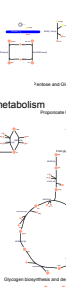
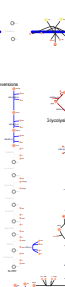
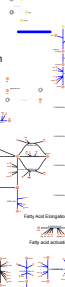
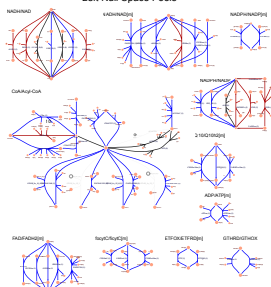
- 1 Orth, J. D. *et al.* A comprehensive genome-scale reconstruction of Escherichia coli metabolism--2011. *Mol Syst Biol* **7**, 535, (2011).
- 2 Reed, J. L., Vo, T. D., Schilling, C. H. & Palsson, B. O. An expanded genome-scale model of Escherichia coli K-12 (iJR904 GSM/GPR). *Genome Biol* **4**, R54, (2003).
- 3 Jamshidi, N. & Palsson, B. O. Investigating the metabolic capabilities of Mycobacterium tuberculosis H37Rv using the in silico strain iNJ661 and proposing alternative drug targets. *BMC Syst Biol* **1**, 26, (2007).
- 4 Oh, Y. K., Palsson, B. O., Park, S. M., Schilling, C. H. & Mahadevan, R. Genome-scale reconstruction of metabolic network in *Bacillus subtilis* based on high-throughput phenotyping and gene essentiality data. *J Biol Chem* **282**, 28791-28799, (2007).
- 5 Brochado, A. R., Andrejev, S., Maranas, C. D. & Patil, K. R. Impact of stoichiometry representation on simulation of genotype-phenotype relationships in metabolic networks. *PLoS Comput Biol* **8**, e1002758, (2012).
- 6 Burgard, A. P., Nikolaev, E. V., Schilling, C. H. & Maranas, C. D. Flux Coupling Analysis of Genome-Scale Metabolic Network Reconstructions. *Genome. Res.* **14**, 301-312, (2004).
- 7 David, L., Marashi, S. A., Larhlimi, A., Mieth, B. & Bockmayr, A. FFCA: a feasibility-based method for flux coupling analysis of metabolic networks. *BMC Bioinformatics* **12**, 236, (2011).
- 8 Kim, D. H. & Motter, A. E. Slave nodes and the controllability of metabolic networks. *New J Phys* **11**, (2009).



Left Null Space Pools



Left Null Space Pools



Alternate carbon metabolism

Redox management

Nucleotide metabolism

IMP Biosynthesis

Heme biosynthesis and degradation

PAF neurotransmitter

Pentose and Glucuronate Interconversions

Propionate Metabolism

Suglycolysis

Pentose Phosphate Pathway

Glycolysis

TCA Cycle

Aspartate metabolism

Glutamate metabolism

Vanine, Leucine, Isoleucine metabolism

Alanine metabolism

Phenylalanine metabolism

Urea cycle

Lysine metabolism

Histidine metabolism

Arginine metabolism

Glutamine metabolism

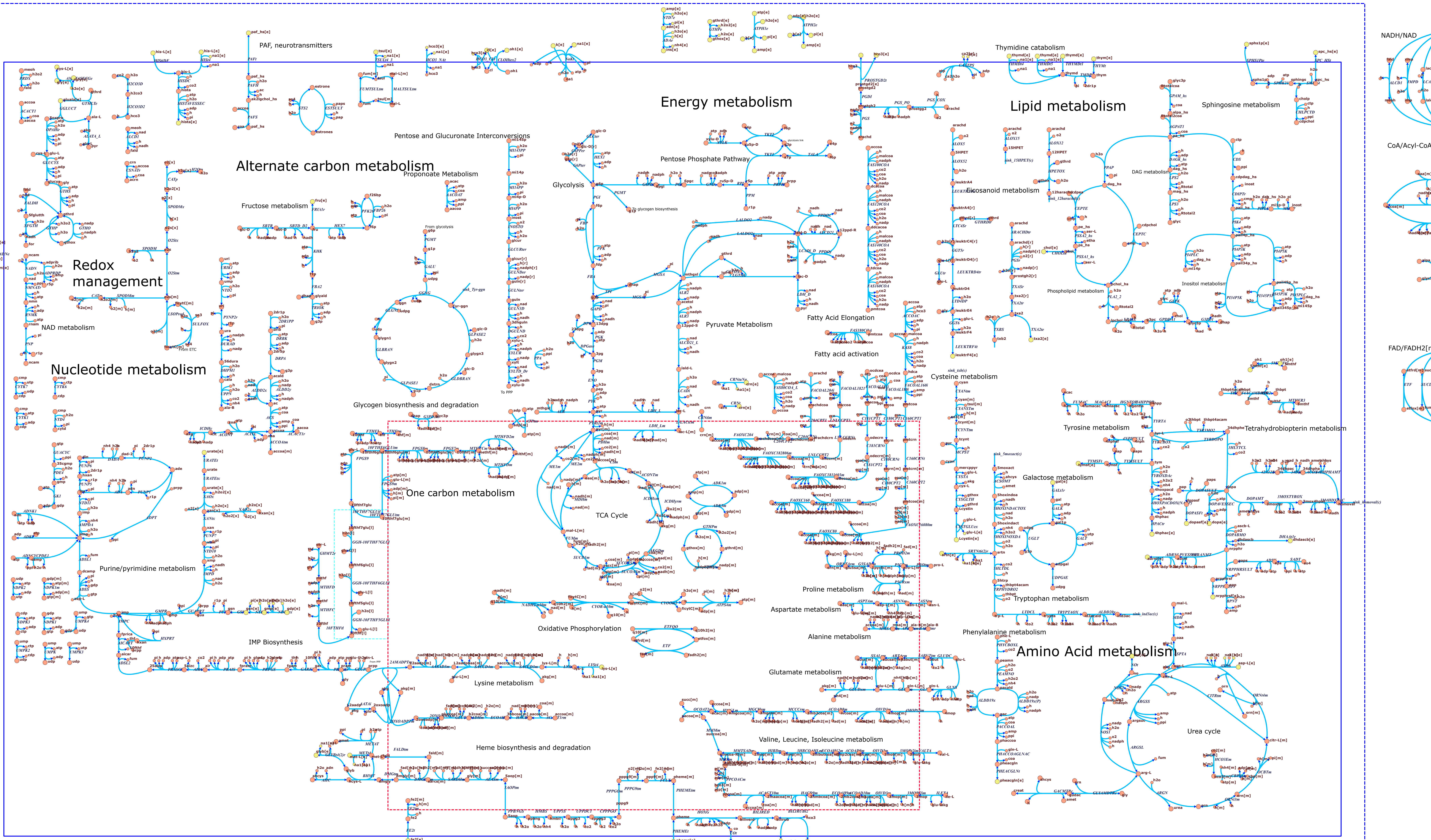
Proline metabolism

Alanine, Aspartate, and Glutamate metabolism

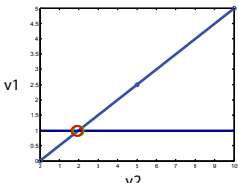
Glutathione metabolism

Cysteine and Methionine metabolism

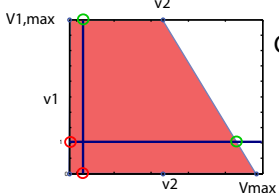
Organic acids



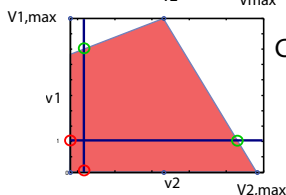
— Flux coupling finder
○ Rmin
○ Rmax



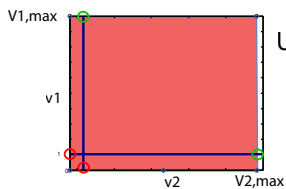
Fully coupled, $R_{\min} = R_{\max}$



Coupled, $R_{\min} \neq 0$ OR $R_{\max} \neq \text{Unbounded}$



Coupled, $R_{\min} \neq 0$ OR $R_{\max} \neq \text{Unbounded}$



Uncoupled: $R_{\min} = 0$; $R_{\max} = \text{Unbounded}$